Evaluation of Detection Range of an Active RFID in Outdoor Environment Using Receiver Diversity with Maximal Ratio Combining

S. P. Majumder and Khalid Mahmud

***Abstract*—An analytic approach is presented to evaluate the Bit Error Rate (BER) and detection range of an active RFID network using space diversity technique both at the reader and the tag receiver. The analysis is carried out with battery powered Application Specific Integrated Circuit (ASIC) type RFID tags for a UWB system with different up-link and down-link frequency ranges. Single Input Multiple Output (SIMO) configuration is used to communicate between the reader and the tag. Maximal Ratio Combining (MRC) technique is used for diversity reception. BPSK, QPSK and M-ary PSK (MPSK) are considered with coherent demodulation to evaluate the BER performance. The results are numerically evaluated and it is found that with the application of the receiver diversity there are significant improvements in BER performance and the maximum detection range achieved with 5 receiving antennas is 920*m* at the BER of 10^{-08}. The maximum improvement in detection range at the same BER with same number of receiving antenna is found to be 361.10*m*. The analyzed approach gives a clear insight regarding the interrelationship between BER, detection ranges,reader received power, number of receiving antenna, order of modulation and detection range improvement and has given improved performance in detecting tag at a comparatively longer distance in outdoor non line of sight (NLOS) environment.**

***Index Terms*—Active RFID, ASIC, BER, duplexer, modulation order, MPSK, MRC, read range.**

I. Introduction

Radio Frequency Identification (RFID) is a wireless data communication technology, which uses Radio Frequency (RF) wave for the communication between the reader and the tag. The data carrying device is called a tag or a transponder. A reader or an interrogator is used to read and write the tag's information [1]. RFID systems are mainly classified as active, semi-active and passive systems depending on whether the tags are powered up by their own power supply or by the RF energy provided by the interrogating signal [2]. An active RFID system uses an internal battery within the tag to continuously power up the tag and its RF communication circuitry. As such, it only requires very low-level signals to be transmitted to the reader. A semi-active tag also contains a battery, but the battery is used only to energize the chip. Unlike the active RFID it does not amplify the signal. Passive RFID tags, on the other hand, have no internal power supply and, therefore, can be much smaller and have an unlimited life span [3]. Passive tags can themselves be classified as chipped and chipless tags and are restricted to relatively small distances to the reader. Passive tags with chips are basically the conventional Application Specific Integrated Circuit (ASIC) RFID tags. Passive tags without chips which is otherwise known as chipless RFID, are attractive because of their low cost and their ability to function at extreme temperature and radiation level [4]. RFID offers NLOS, long distance and all weather reading with the data carrying capacity larger than an optical barcode can offer. Over the past few years this massively expanding technology have drawn considerable attention in the microwave community due to its use in a diversity of applications namely communication, ticketing, transportation, logistics, tracking, Inventory management, human identification, security, retail stock management, parking access control, toll collection, healthcare , etc. [5].

To the authors' best knowledge, the frequency division active tags [6] are yet to be widely analyzed for long range (1000*m* and above) detection. Therefore in this paper an analytic approach is presented to evaluate the detection range of an active RFID in outdoor environment using receiver diversity both in the reader and the tag using MRC for Rayleigh fading over the channels. Results are evaluated numerically for different environment using BPSK, QPSK and MPSK modulation scheme and improvements in detection range is evaluated for different diversity conditions. The background and related workshave been explained in Section II, the system model has been explained in Section III, the analysis part is explained in Section IV, in Section V the results are discussed and finally in Section VI concluding remarks are added along with the scopes of future developments.

II. Related Works

Since an active RFID tag involves the incorporation of power sources with the passive one, the significance of the researches and other developments carried out for the improvements of detection range of passive RFID tags are equally applicable for the active one. Battery-powered active tag typically has a detection range of 300 feet (100m) while the passive one has detection range less than 50m [7], [8]. Some of the significant research works that involves improvement of the detection range of the RFID system are given below:

Manuscript received October 16, 2014; revised January 6, 2015.

S. P. Majumderis with the Electrical and Electronic Engineering Department, Bangladesh University of Engineering and Technology, Dhaka, Bangladesh (e-mail: spmajumder@eee.buet.ac.bd).

Khalid Mahmud is with the Electrical and Electronic Engineering Department, Bangladesh University of Engineering and Technology, Dhaka, Bangladesh. He is also with Military institute of Science and Technology, Bangladesh (e-mail: khalidarmy@dhaka.net).

In reference [9] the range of the ultra-wideband transmission system has been improved using rake receiver where the transmitter to receiver distance (Round trip distance) is found to be less than 100m. In [10] a detection range of $60m$ was achieved using bi-static backscatter radio architecture with the carrier emitter placed at the center of the Backscatter Sensor Network (BSN) "cell" and tags located around it. However, in the experiment each tag was powered up by a low-cost photovoltaic cell that consumed $0.5mW$ of power. Another Surface Acoustic Wave (SAW) based tag detection technique is introduced in [11] where a maximum detectionrange of $30m$ could be achieved. In [12] wireless measurement of various physical quantities from the analysis of the RADAR Cross Sections (RCS) variability of passive electromagnetic sensors have been presented where a maximum detection range of $30m$ is achieved. In [13] a general model for UWB channels has been presented that is valid for the high frequency range ($3GHz-10\,GHz$) in a number of different environments as well as for the frequency where the maximum distance achieved is about $28m$. In [14] a very comprehensive study has been done regarding the detection range of chipless RFID, although the maximum range repeatedly acknowledged here remained below $10m$.

III. System Model

The system is composed of a reader (Interrogator) and a battery powered ASIC type active tag (Active sensor tag) each equipped with an antenna serving the purpose of both transmitter and receiver simultaneously with the help of duplexers (An antenna duplexer or RF duplexer is a unit that can be used to enable more than one transmitter and receiver to operate on a single RF antenna [15]) as shown in Fig. 1. During the up-link transmission when the interrogation signal from the reader reaches the active tag, it is received using the receiving antennas of the tag and propagates further on towards the battery powered ASIC, attached to the tag. The ASIC encodes data bits introducing attenuation and phase jumps at particular frequencies of the spectrum. After passing through the ASIC, the signal containing the unique spectral signature of the tag is transmitted back to the reader receivers during the down-link transmission.

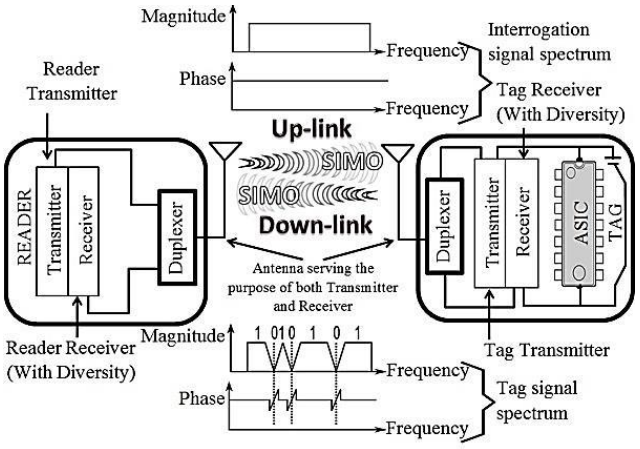

Fig. 1. System model.

In the transmitter section of Fig. 2, the interrogator signal passes through a band pass filter (BPF) which acts as an input band limiting device. The band limited signal then goes through an up-converter which converts the frequency of the interrogating signal to a suitable frequency. The up-converted signal is then passed through the high power amplifier (HPA) that amplifies the modulated RF carrier to a suitable level [16]. On the receiver section of Fig. 2, the reader receives the low-level modulated RF carrier in the down-link frequency spectrum. The low noise amplifier (LNA) is used to amplify the weak received band limited signals and improve the signal to noise ratio (SNR). RF is then re-converted to IF by the down-converter. The demodulator estimates which of the possible symbols were transmitted based on observation [17].

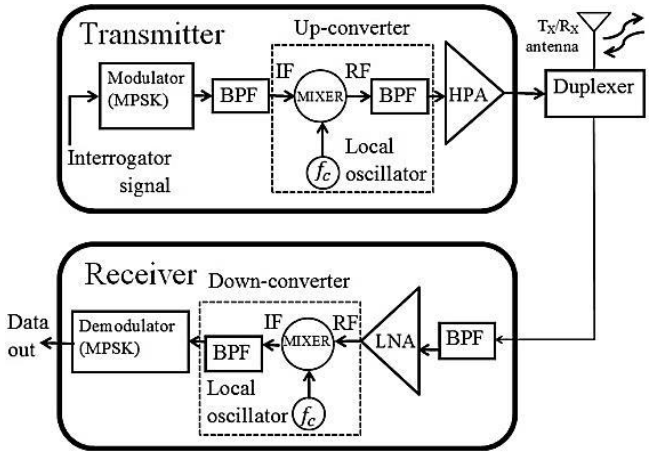

Fig. 2. Transmitter/receiver block diagram.

After obtaining independently faded signal components at the output of the demodulators, MRC technique is used to combine these signal components for transmitted symbol detection. In MRC each signal branch is multiplied by a weight factor that is proportional to the signal amplitude. That is, branches with strong signals are further amplified, while weak signals are attenuated. If we consider a transmission of a digital modulated signal $x(t)$ over flat slow Rayleigh fading channels using coherent demodulation with Lth order diversity. The received component from the lth diversity channel is expressed as below:

$$r_l(t) = \alpha_l(t)\exp[j\,\theta_l(t)]x(t) + w_l(t), \quad l = 1, 2, 3 \qquad (1)$$

Here, $w_l(t)$ is assumed to be the Additive White Gaussian Noise (AWGN). In MRC, the combining technique assumes that the receiver is able to accurately estimate the amplitude fading $\alpha_l(t)$ and carrier phase distortion $\theta_l(t)$ for each diversity channel. With the knowledge of complex channel gains, $\alpha_l(t)e^{j\theta_l(t)}$, l=1, 2, ..., L, the receiver coherently demodulates the received signal from each branch. The phase distortion $\theta_l(t)$ of the received signal is removed from the lth branch by multiplying the signal component by $e^{-j\theta_l(t)}$. The coherently detected signal is then weighted by the corresponding amplitude gain, $\alpha_l(t)$. The weighted received signals from all the L branches are then summed together and applied to the decision device to achieve the best performance [18]. Fig. 3 shows an example of the application of MRC technique in the reader receiver. Same diversity technique is applicable for the tag receiver.

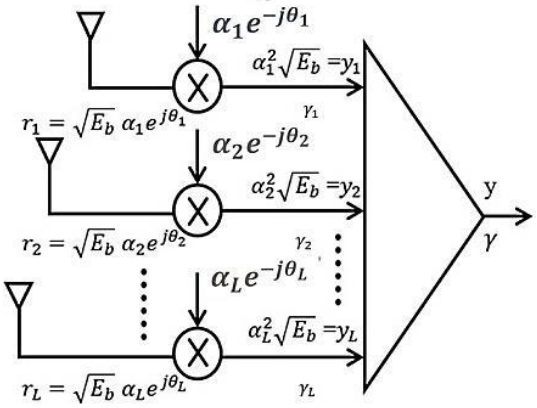

Fig. 3. Diversity reception with maximal ratio combining.

IV. Analysis

Since transmission and reception is being done by separate up-link and down-link frequencies the analysis is therefore carried out in two steps (Up-link and Down-link). During up-link the reader acts as the transmitter while the tag acts as the receiver and during down-link transmission the tag acts as the transmitter and the reader acts as the receiver. Details are given below:

The transmitted signal from reader and tag for up-link transmission in case of a coherent MPSK modulation can be expressed as below [19]:

$$s_i(t) = A(t)\cos[2\pi f_c t + \theta_i(t)], \quad 0 \le t \le T, i = 1,2 \cdots M \tag{2}$$

Here, $A(t)$ is the amplitude and $\theta_i(t)$ is the carrier phase distortion, and $\theta_i = \frac{2i-1}{M}\cdot\pi$. M is chosen as a power of 2 (i.e., $M = 2^n$ or $n = log_2 M$) . In case of $M \le 4$ it is more appropriate to apply BPSK/QPSK modulation technique. Hence the transmitted signal in case of both coherent BPSK and QPSK modulation can be expressed as below [20]:

$$s(t) = A(t)\cos[2\pi f_c t + \varphi(t)], \quad 0 \le t \le T \tag{3}$$

Here, $A(t)$ is the amplitude and $\varphi(t)$ is the phase of the modulated signal. for BPSK, $\varphi(t) = \pm\pi$ and for QPSK, $\varphi(t) = \pm\frac{\pi}{4}, \pm\frac{3\pi}{4}$. The signal received by reader/tag receiver is given by:

$$\begin{aligned} r(t) &= s_i(t)\otimes g(t) + n(t) \\ r(t) &= s(t)\otimes g(t) + n(t) \end{aligned} \tag{4}$$

The generalized expression of the signal received by the reader/tag receiver with $j-th$ antenna in case of MPSK, BPSK or QPSK is given by:

$$\begin{aligned} y_j(t) &= r(t)\otimes h_j(t) + n_0(t) \\ &= s(t)\otimes g(t)\otimes h_j(t) + n(t) \end{aligned} \tag{5}$$

The output of the maximal ratio combiner is [21]:

$$y_0(t) = \sum_{j=i}^{L} y_{j(t)}\otimes h_j^*(t) + n_0(t)$$

$$= \sum_{j=i}^{L} s(t)\otimes g(t) \times |h_j(t)^2| + n_0(t) + n(t) \tag{6}$$

$g(t)$ Includes the effect of channel gain coefficient and $h_j(t)$ is the channel gain for the tag to $j-th$ receiver. Frequency dependent path gain, $g(t)$ in a UWB environment neglecting the interdependence between the direction of the radiation and the directivity of the antennas for up-link transmission is expressed as follows [13]:

$$\begin{aligned} G(f)_{U/L} &= \frac{P_{RX,tag}}{P_{TX,rdr}} \\ &= \frac{1}{2}\cdot G_0 \cdot \eta_{TX,rdr}\eta_{RX,tag} \cdot \frac{\left(\frac{f}{f_c}\right)^{-2(k+1)}}{\left(\frac{d}{d_0}\right)^n} \end{aligned} \tag{7}$$

Here, $f_{min,U/L}$ = Minimum frequency for up-link transmission, $f_{max,U/L}$ = Maximum frequency for up-link transmission, $BW_{U/L}$ = Band Width for up-link transmission, $f_{c,U/L}$ = Reference frequency for up-link transmission, d = Distance in meter, d_0 = Reference distance, $P_{TX,rdr}$ = Reader transmit power, $G(f)_{U/L}$ = Path gain=$\frac{P_{RX,tag}}{P_{TX,rdr}}$, $P_{RX,tag}$ = Tag receive power, G_0 = Path loss in reference distance in dB, $\eta_{TX,rdr}$ = Reader antenna transmit efficiency, $\eta_{RX,tag}$ = Tag antenna receive efficiency, k = Decaying factor and n = Path loss exponent. By furnishing all the necessary data in equation 7, $P_{RX,tag}$ is calculated. Thereafter, $P_{RdBm,tag}$ is calculated using the formula $P_{RdBm,tag} = 30 + 10 \times log10(P_{RX,tag})$. The conditional bit error probabilities for an MPSK, BPSK and QPSK system are given as follows [19]:

$$\begin{aligned} P_{b,tag}(\gamma)_M &= \frac{1}{log_2 M}\cdot erfc\cdot\sqrt{\frac{E_{b,tag}log_2 M}{N_0}}\,sin\frac{\pi}{M} \\ P_{b,tag}(\gamma)_B &= \frac{1}{2}\cdot erfc\cdot\sqrt{\frac{E_{b,tag}}{N_0}} \\ P_{b,tag}(\gamma)_Q &= \frac{1}{2}\cdot erfc\cdot\sqrt{\frac{E_{b,tag}}{N_0}} \end{aligned} \tag{8}$$

Here Energy pet bit, $E_{b,tag} = P_{RX,tag} \times T_{P,U/L}$. The subscriptions M, B and Q denotes MPSK, BPSK and QPSK modulation scheme respectively. By furnishing the data in equation 8, $P_{b,tag}(\gamma)$ is calculated. Probability density function in a Rayleigh fading environment using MRC technique is given below [18]:

$$P_{r,tag}(\gamma) = \frac{\gamma^{L-1}\times exp^{-\left(\frac{\gamma}{\gamma_{c,tag}}\right)}}{(L-1)!\times\gamma_{c,tag}^{L}} \tag{9}$$

Here the average SNR per bit in each diversity channel, $\gamma_{c,tag} = \frac{P_{RX,tag}\times T_{P,U/L}}{N_0}$, L = Number of receiving antenna, Time gap between two adjacent pulses, $T_{P,U/L} = \frac{1}{BW_{U/L}}$, Noise power spectral density, $N_0 = K \times T \times F$, K = Boltzmann constant , T = Room temperature, F = Noise figure and γ =

Overall signal to noise ratio. By furnishing the data in equation 9, $P_{r,tag}(\gamma)$ is calculated. The average BER with Rayleigh fading over the channels with diversity can be expressed as follows:

$$BER_{(tag)M} = \int_0^\infty P_{b,tag}(\gamma)_M \cdot P_{r,tag}(\gamma)dx$$
$$BER_{(tag)B} = \int_0^\infty P_{b,tag}(\gamma)_B \cdot P_{r,tag}(\gamma)dx \quad (10)$$
$$BER_{(tag)Q} = \int_0^\infty P_{b,tag}(\gamma)_Q \cdot P_{r,tag}(\gamma)dx$$

The analysis carried out for down-link transmission is exactly similar to that followed in case of the up-link transmission with only one exception in regards to the operating mode of the tag which in this case acts as transmitter while the reader taking over the role of the receiver. Details are given below:

$$G(f)_{D/L} = \frac{P_{RX,rdr}}{P_{TX,tag}}$$
$$= \frac{1}{2} \cdot G_0 \cdot \eta_{TX,tag}\eta_{RX,rdr} \cdot \frac{\left(\frac{f}{f_c}\right)^{-2(k+1)}}{\left(\frac{d}{d_0}\right)^n} \quad (11)$$

Here, $f_{min,D/L}$ = Minimum frequency for down-link transmission, $f_{max,D/L}$ = Maximum frequency for down-link transmission, $BW_{D/L}$ = Band width for down-link transmission, $f_{c,D/L}$ = Reference frequency for down-link transmission, d = Distance in meter, d_0 = Reference distance, $P_{TX,tag}$ = Tag transmit power, $G(f)_{D/L}$= Path gain=$\frac{P_{RX,rdr}}{P_{TX,tag}}$, $P_{RX,rdr}$ = Reader received power, G_0 = Path loss in the reference distance in dB, $\eta_{TX,tag}$ = Tag antenna transmit efficiency, $\eta_{RX,rdr}$ = Reader antenna receive efficiency, k = Decaying factor and n = Path loss exponent. By furnishing all the necessary data in equation 11, $P_{RX,rdr}$ is calculated. Thereafter, $P_{RdBm,rdr}$ is calculated using the formula $P_{RdBm,rdr} = 30 + 10 \times log10(P_{RX,rdr})$. The conditional bit error probability for an MPSK, BPSK and QPSK system are given as follows:

$$P_{b,rdr}(\gamma)_M = \frac{1}{log_2 M} \cdot erfc \cdot \sqrt{\frac{E_{b,rdr} log_2 M}{N_0}} sin\frac{\pi}{M}$$
$$P_{b,rdr}(\gamma)_B = \frac{1}{2} \cdot erfc \cdot \sqrt{\frac{E_{b,rdr}}{N_0}} \quad (12)$$
$$P_{b,rdr}(\gamma)_Q = \frac{1}{2} \cdot erfc \cdot \sqrt{\frac{E_{b,rdr}}{N_0}}$$

Here Energy pet bit, $E_{b,rdr} = P_{RX,rdr} \times T_{P,D/L}$. By furnishing the data in equation 12, $P_{b,rdr}(\gamma)$ is calculated. Probability density function in a Rayleigh fading environment using MRC technique is given as follows:

$$P_{r,rdr}(\gamma) = \frac{\gamma^{L-1} \times exp^{-\left(\frac{\gamma}{\gamma_{c,rdr}}\right)}}{(L-1)! \times \gamma_{c,rdr}^L} \quad (13)$$

Here the average SNR per bit in each diversity channel, $\gamma_{c,rdr} = \frac{P_{RX,rdr} \times T_{P,D/L}}{N_0}$, L = Receiving antenna, Time gap between two adjacent pulse, $T_{P,D/L}$ = $\frac{1}{BW_{D/L}}$, Noise power spectral density, $N_0 = K \times T \times F$, K = Boltzmann constant , T = Room temperature, F = Noise figure and γ = Overall signal to noise ratio. By furnishing the data in equation 13, $P_{r,rdr}(\gamma)$ is calculated. The average BER with Rayleigh fading over the channels with diversity can be expressed as follows:

$$BER_{(rdr)M} = \int_0^\infty P_{b,rdr}(\gamma)_M \cdot P_{r,rdr}(\gamma)dx$$
$$BER_{(rdr)B} = \int_0^\infty P_{b,rdr}(\gamma)_B \cdot P_{r,rdr}(\gamma)dx \quad (14)$$
$$BER_{(rdr)Q} = \int_0^\infty P_{b,rdr}(\gamma)_Q \cdot P_{r,rdr}(\gamma)dx$$

The total BER is calculated form the BER values of the reader and tag found out in equation 10 and equation 14.

$$BER_M = \frac{1}{2} \cdot [BER_{(rdr)M} + BER_{(tag)M}]$$
$$BER_B = \frac{1}{2} \cdot [BER_{(rdr)B} + BER_{(tag)B}] \quad (15)$$
$$BER_Q = \frac{1}{2} \cdot [BER_{(rdr)Q} + BER_{(tag)Q}]$$

V. Results and Discussion

In the outdoor environments with a good number of propagation obstacles in between, the delay spread is expected to remain small compared to other environments. For up-link transmission, we assumed, $P_{TX,rdr}$ = $0.5W$ (fixed), Other parameters are assumed as, $f_{\text{min,U/L}}$ = 3GHz, $f_{\text{max,U/L}}$ = $6GHz$, $f_{\text{c,U/L}}$ = $5GHz$, $BW_{\text{U/L}}$ = $500MHz$, G_0 = $-50dB$, d_0 = $1m$, $\eta_{TX,rdr}$ = 0.80, $\eta_{RX,tag}$ = 0.20, n = 1.58 and k = 0. For down-link transmission, we assumed $P_{TX,tag}$ = $1mW$, other parameters are assumed as, $f_{\text{min,D/L}}$ = $868MHz$, $f_{max,\text{D/L}}$ = $915MHz$, $f_{\text{c,D/L}}$ = $500Mz$, $BW_{\text{D/L}}$ = $100KHz$, G_0 = $-50dB$, d_0 = $1m$, $\eta_{TX,tag}$ = 0.80, $\eta_{RX,rdr}$ = 0.20, n = 1.58, and k = 0. The parameters for up-link transmission have already been used in previous analysis in a research work and have been accepted as standardized model by IEEE 802.15.4a [13] and the parameters for down-link transmission in case of an active tag is taken from GAO RFID inc(GAO RFID Inc. has established itself as one of world's most influential suppliers of RFID products, including RFID tags, readers and software, as well as integrated solutions for various vertical markets) which is already in mass production (Active RFID UHF Beacon Tag 137001) [22] and carrying reputed entity in different fields of RFID. Following the analysis presented in section IV, the BER performance of an RFID network is evaluated numerically with respect to many other parameters for read range improvement. Details are described in the succeeding paragraphs:

A. Fixed Transmit Power of Reader and Tag

The plots of BER versus power received by the reader receiver are shown in Fig. 4, for outdoor NLOS environment with diversity in the reader and tag receiver. It is noticed that

the receiver sensitivity at a given BER improves (Received power decreases) with the increase of the number of receiving antenna at a given transmit power level. It is further noticed that at a fixed number of receiving antenna BER decreases with the increase of received power. Analysis is carried out with both BPSK and QPSK modulation technique and similar results are found for both of them (For similar bit error probability as shown in equation 8 and 12).

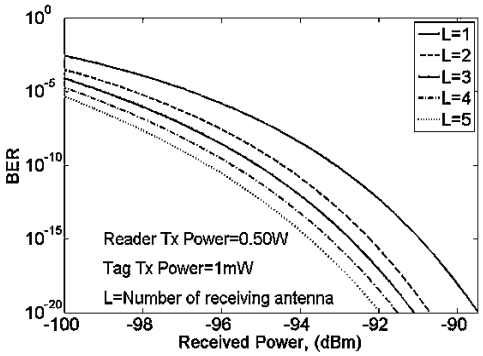

Fig. 4. BER versus tag received power $P_{RX}(dBm)$.

Fig. 5 depicts the plots of BER versus distance achieved by an active RFID system in outdoor NLOS environment for different receive antenna diversity. From the plot it is clear that the BER increases with the increase of distance for a given number of antennas. It is further noticed that as the number of receiving antenna in increased, the achievable distance is increased at the same BER.

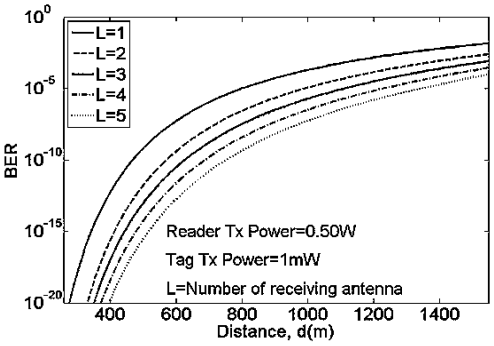

Fig. 5. BER versus distance,$d(m)$.

Both the results achieved from Fig. 4 and Fig. 5 are elaborately furnished in Table I for different number of receiving antenna with fixed transmit power applied in the reader and the tag, where it is found that there is a significant improvement in achievable distance and receiver sensitivity with the increase of the number of the receiver antenna.

Fig. 6 shows the plots of reader received power $P_{\mathrm{RX,reader}}$ versus number of receiving antenna, L. Here it is shown that the reader received power decreases (receiver sensitivity improves) with the increase of the number of receiving antenna. It is further noticed that for a particular number of receiving antenna received power increases (receiver sensitivity decreases) with the decreases of BER

Fig. 7 shows the plots of distance, $d(m)$ versus number of receiving antenna L. Here it is shown that the detection distance of the reader increases with the increase of the number of receiving antenna. It is further noticed that for a particular number of receiving antenna detection range increases with the increase of BER.

TABLE I: RECEIVER SENSITIVITY AND DISTANCE AT A GIVEN BER WITH FIXED TRANSMIT POWER AND DIFFERENT NUMBER OF ANTENNA (OUTDOOR NLOS ENVIRONMENT, BPSK/QPSK)

Received Power in dBm for Different L					
BER	$L=1$	$L=2$	$L=3$	$L=4$	$L=5$
10^{-08}	-94.28	-95.68	-96.39	-97.07	-97.72
10^{-10}	-93.08	-94.43	-95.08	-95.71	-96.33
10^{-12}	-92.11	-93.43	-94.01	-94.59	-95.17
10^{-14}	-91.31	-92.59	-93.12	-93.65	-94.19
10^{-16}	-90.62	-91.88	-92.35	-92.84	-93.33
10^{-18}	-90.01	-91.25	-91.69	-92.12	-92.60
Distance in meter for Different L					
BER	$L=1$	$L=2$	$L=3$	$L=4$	$L=5$
10^{-08}	559.30	684.90	758.10	839.50	920.40
10^{-10}	468.10	571.80	626.30	686.60	752.30
10^{-12}	407.30	493.40	536.10	585.40	636.30
10^{-14}	362.10	437.10	471.00	509.10	550.40
10^{-16}	326.90	393.40	421.50	452.60	486.90
10^{-18}	299.40	359.20	382.30	408.40	436.50

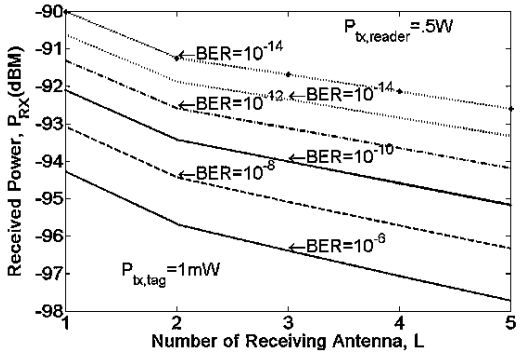

Fig. 6. Received power, $P_{RX}(dBm)$versus no of receiving antenna, L.

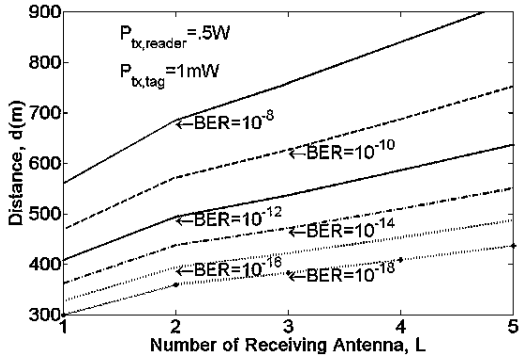

Fig. 7. Distance, $d(m)$ versus no of receiving antenna, L.

Fig. 8 shows the plots of improvement of reader received power versus number of receiving antenna. Here gradual improvement of received power is noticed with the gradual increment of the number of receiving antennas. Besides, at a particular number of receiving antenna the magnitude of the improvement in received power seems to be more significant at higher BER.

Fig. 9 shows the plots of improvement of distance versus number of receiving antenna. This figure clearly shows that the improvement is more with more number of receiving antennas and the improvement is more significant at higher BER.

The values of the received power are plotted in Fig. 10 as a function of number of reader antenna, L for a specific value of BER (10^{-10}) for different values of M ($M = 8,16,32,64,128$). From this plot two significant features can

be deduced. Firstly the value of the received power decreases (receiver sensitivity increases) with the increase of the receiver antenna and received power increases (receiver sensitivity decreases) as the modulation order is increased for a particular number of receiving antenna.

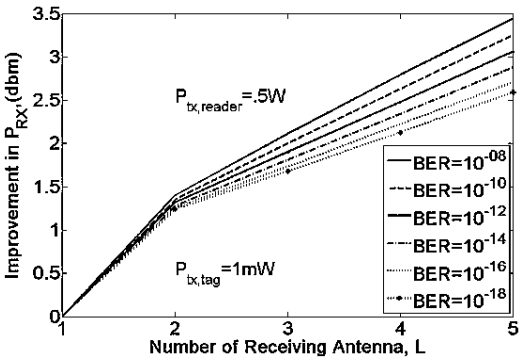

Fig. 8. Improvement in received power $P_{RX}(dBm)$ versus, L.

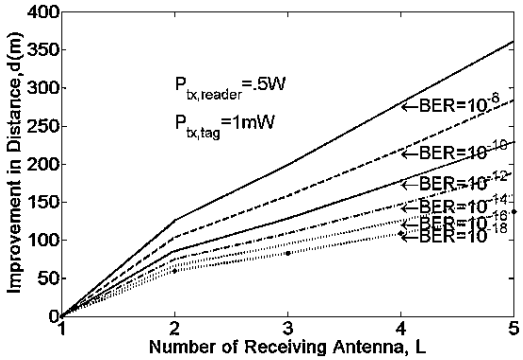

Fig. 9. Improvement in distance, $d(m)$ versus no of receiving antenna, L.

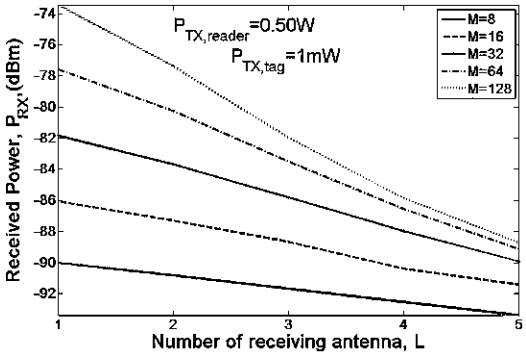

Fig. 10. Received power, $P_{RX}(dBm)$ versus no of receiving antenna, L.

The achievable values of the distance are also plotted in Fig. 11 as a function of number of reader receiver antenna, L for a specific value of BER (10^{-10}) for different values of $M(M = 8,16,32,64,128)$. From the analysis it is noticed that, achievable distance is however smaller for higher values of M and bigger for lower values of M. This is because higher-order modulations (i.e. large) are more spectrally efficient but less power efficient (i.e. BER higher) [23].

Both the results achieved from Fig. 10 and Fig. 11 are elaborately furnished in Table II for different number of receiving antenna with a fixed transmit power, where it is found that there is a significant decrease in achievable distance and receiver sensitivity with the increase of the number of the modulation order. However the findings are very important since higher order modulation improves spectral efficiency allowing substantial uplift in data handling capacity.

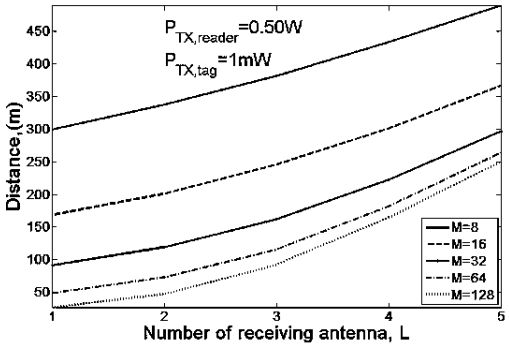

Fig. 11. Distance, $d(m)$ versus no of receiving antenna, L.

TABLE II: RECEIVER SENSITIVITY AND DISTANCE FOR DIFFERENT MODULATION ORDER AT A GIVEN BER OF 10^{-10} WITH FIXED TRANSMITTER AND RECEIVER POWER AND DIFFERENT NUMBER OF ANTENNAS

Received Power in dBm for Different L					
BER	$L=1$	$L=2$	$L=3$	$L=4$	$L=5$
$M=8$	-90.01	-90.83	-91.68	-92.53	-93.39
$M=16$	-86.08	-87.30	-88.67	-90.40	-91.41
$M=32$	-81.84	-83.69	-85.79	-87.96	-89.92
$M=62$	-77.59	-80.27	-83.51	-86.56	-89.13
$M=128$	-73.46	-77.39	-81.97	-85.88	-88.72
Distance in meter for Different L					
BER	$L=1$	$L=2$	$L=3$	$L=4$	$L=5$
$M=8$	299.50	337.60	382.20	433.50	489.90
$M=16$	168.50	201.60	245.90	301.30	366.60
$M=32$	91.44	119.60	162.30	222.60	296.60
$M=62$	49.09	73.20	115.90	181.90	263.90
$M=128$	27.17	47.89	92.76	164.40	250.00

Finally, Fig. 12 depicts the plots of maximum allowable distance for different diversity scheme. Results obtained from these plots provides an at a glance idea regarding the maximum read range at different BER at different number of antennas that helps in choosing the appropriate optionfor the appropriate requirement. Here it is noticed that a maximum distance of $920.40m$ is achieved at the BER of 10^{-08} using 5 receiving antenna. The improvement achieved from 1 receiving antenna to 5 receiving antenna appears to be $361.10m$ at the same BER.

B. Fixed Reader and Variable Tag Transmit Power

The plots of BER versus distance for outdoor environment with 5 receiving antenna are shown in Fig. 13, with transmit power as a parameter. The plots indicate that for a given transmit power the BER increases as the distance is increased. It further indicates that for a given distance the value of BER decreases (BER improves) with the increase of transmitted power.

The plots shown in Fig. 14 indicate the achievable distance for a given BER as a function of transmit power. These plots clearly indicate that the maximum achievable distance is however lower at lower BER. The plots further reveals that for a fixed transmit power achievable distance improves as the BER increases.

C. Comparison with Existing Research Works/Products

The maximum achievable detection range analytically

evaluated in the proposed systm as discussed in Section V of this paper is $920.40m$ at the BER of 10^{-08}. To the authors best knowledge a research work obtaining such long detection range has not been done yet. The application of space diversity with MRC makes the overall procedure simple, straightforward and easy to implement. Besides most of the active RFID tags practically available in the market today have detection distance lower than that evaluated in this paper. A comparative study, shown in Table III reveals the fact [22], [24]-[26].

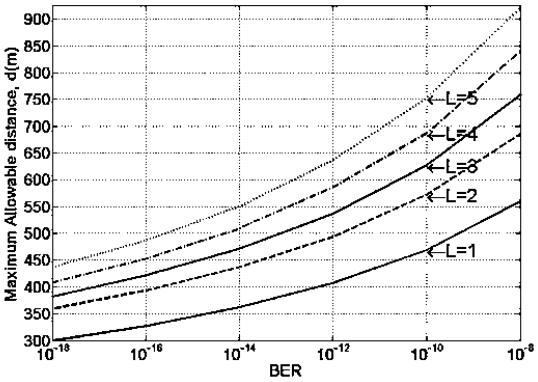

Fig. 12. Distance, $d(m)$ versus no of receiving antenna, L.

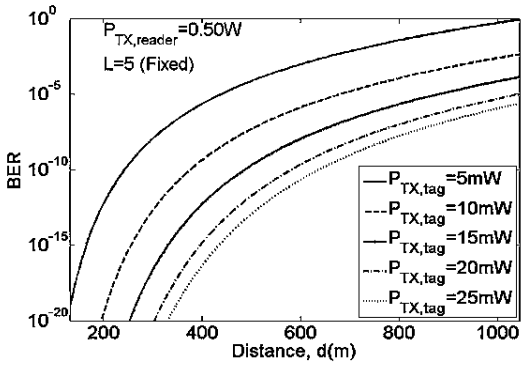

Fig. 13. BER versus distance, $d(m)$.

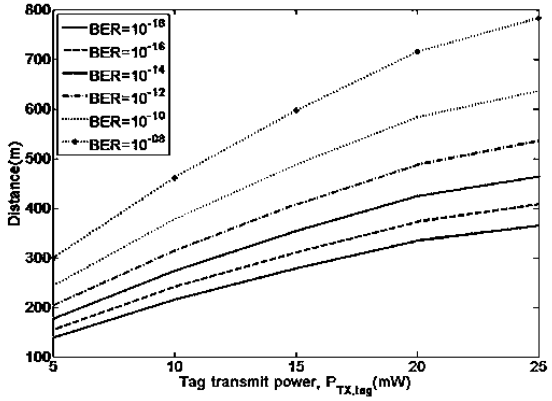

Fig. 14. Distance, $d(m)$ versus tag transmitted power, $P_{TX,tag}(dBm)$.

TABLE III: SOME ACTIVE TAGS WITH THEIR COUNTRY OF ORIGIN

Brand	Company of Origin	Detection range
Onmi-ID Active Tag	USA	400m
GAO RFID tag 127004	USA & Canada	100m
Wavetreand-Tag (TGP)	UK	100m
GSIT	Chania (Mainland)	100m
Nexqo	Chania (Mainland)	80m
TZONE	Chania (Mainland)	50m

VI. CONCLUSION

A low-cost architecture and a simple analysis method for detecting ASIC-based active RFID tags in UWB for outdoor NLOS environment using MRC technique is presented. It is found that the detection range can be increased significantly by increasing the number of receiving antenna at the reader receiver without increasing the transmit power. The introduction of BPSK, QPSK and MPSK modulation scheme with different spectral efficiency has provided additional option for handling more data with compromised detection range. RFID technology is still evoking plenty of scopes for its improvements. For future advancements MIMO Orthogonal Frequency Division Multiplexing (OFDM) technology can be used with the application of transmitter diversity. This paper focuses only on receiver diversity. Therefore the combined application of transmitter and receiver diversity is expected to give a much better result. OFDM technique is widely used in wireless communication in many applications due to its good spectral performance and low sensitivity to impulse noise and multipath channels [27]. For coherent demodulation the application of PPM technique instead of MPSK may improve the detection range. GPS enabled active RFID tag [28] or incorporating cellular technology into active tag [29] can also bring substantial improvement in tag detection range. However, considering all the pros and cons, the proposed method explained in this paper not only offers an easy way to evaluate detection range but also possess countless potentials to make industrial breakthrough in different sectors such as building management, field service, fleet maintenance, industrial laundry, Industrial Painting, livestock, marinas oil & gas industry, people tracking, railway, etc. where long range detection can give an abrupt uplift in the overall system.

ACKNOWLEDGEMENT

This paper is the outcome of the M.Sc. in Electrical and Electronic Engineering program running in Bangladesh University of Engineering and Technology (BUET), Dhaka, Bangladesh.We express our sincere gratitude to theteachers and technical staffs of BUETwho has given valuable advice and whole hearted support in making this analytic paper a successful one.

REFERENCES

[1] K. Finkenzeller, *RFID Handbook: Fundamentals and Applications in Contactless Smart Cards and Identification*, 2nd ed., Hoboken, NJ: Wiley, 2003.

[2] R. V. Koswatta, "Readers for frequency signature-based chipless RFID tags," PhD thesis, Department of Electrical and Computer Systems Engineering Monash University, Australia, March 2013.

[3] R. V. Koswatta and N. C. Karmakar, "A novel reader architecture based on UWB chirp signal interrogation for multiresonator based chipless RFID tag reading," *IEEE Transcation on Microwave Theory and Techniques*, vol. 60, no. 9, September 2012.

[4] S. Preradovic and N. C. Karmakar, "Multiresonator-based chipless RFID," *Barcode of the Future*, Springer, 2012.

[5] S. Preradovic, I. Balbin, N. C. Karmakar, and G. F. Swiegers, "Multiresonator-based chipless RFID system for low-cost item tracking," *IEEE Trans. Microw. Theory Techn*, vol. 57, no. 5, pp. 1411-1419, May 2009.

[6] M. S. Bhuiyan, R. Azim, and N. Karmakar, "A novel frequency reused based ID generation circuit for chipless RFID applications," in *Proc. Asia-Pacific Microw. Conf*, pp. 14701473, 2011.

[7] R. Weinstein, "RFID: A technical overview and its application to the enterprise," *IEEE Computer Society*, pp. 1520-9202, May-June 2005.

[8] D. Seetharam and R. Fletcher, "Battery-powered RFID," Tag Sense Inc, 2006.
[9] S. Gaur and A. Annamalaj, "Improving the range of ultrawideband transmission using rake receivers," *IEEE*, pp. 7803-7954, 2006.
[10] E. Kampianakis, S. D. Assimonis, and A. Bletsas, "Network demonstration of low-cost and ultra-low-power environmental sensing with analog backscatter," *ECE Dept*., Technical University of Crete, Chania, 2013.
[11] A. Hashemi, A. H. Sarhaddi, and H. Emami, "A review on chipless RFID tag design," *Majlesi Journal of Electrical Engineering*, February 6, 2013.
[12] A. Herv, C. Franck, J. Mehdi, T. Trang, H. Hamida, T. Anya, B. Sofiene, R. Ayoub, P. Patrick, and M. P. T. Manos, "Wireless sensing and identification based on RADAR cross sections variability measurement of passive electromagnetic sensors," *Annals of Telecommunications*, vol. 68, no. 7-8, pp. 425-435, February 6, 2013.
[13] A. F. Molisch, D. Cassioli, C. C. Chong, S. Emami, A. Fort, B. Kannan, J. Kunisch, H. Gregory, Schantz, K. Siwiak, and M. Z. Win, "A comprehensive standardized model for ultrawideband propagation channels," *IEEE Transaction on Antenna and Propagation*, vol. 54, no. 11, 2006.
[14] B. Shao, "Fully printed chipless RFID tags towards item-level tracking applications," PhD thesis, Electronic and Computer Systems (ECS), School of Information and Communication Technology (ICT), Royal Institute of Technology (KTH)Stockholm, Sweden, 2014.
[15] A. Chinig, J. Zbitou, A. Errkik, A.Tribak, H. Bennis, and M. Latrach, "Microstrip triangular loop resonator duplexer," *International Journal of Computer and Communication Engineering*, vol. 2, no. 4, July 2013.
[16] A. Kartz, "Linearizing high power amplifiers," Linearizer Technology Inc., 2013.
[17] H. Hausman, "Fundamentals of satellite communications-part II, link analysis, transmission, path, loss and reception," MITEQ, Inc., 2009.
[18] J. W. Mark and W. Zhuang, *Wireless Communication and Networking*, New Delhi: PHI Learning Private Limited, 2008, ch. 4, pp. 121-129.
[19] F. Xiong, *Digital Modulation Techniques*, 2nd ed., Artech House Telecommunications Library, 2006.
[20] S. Nakahara, *Technologies and Services on Digital Broadcasting*, CORONA Publishing co., Ltd. and NHK, Spring 2003.
[21] S. Haykin, *Communication Systems*, 4th ed., Jhon Wiley and Sons Inc, 2001.
[22] GAO RFID INC. (2014). A member of GAO group. [Online]. Available: http://www.gaorfid.com
[23] R. Suthar, S. Joshi, and N. Agrawal, "Performance analysis of different M-ary modulation techniques in cellular mobile communication," *IP Multimedia Communications a Special Issue from IJCA*, 2009.
[24] Omni ID. (2014). Identify with innovation. [Online]. Available: http://www.atlasrfidstore.com
[25] (2014). Personnel Tag (TGP). [Online]. Available: www.wavetrend.net
[26] L. Yuan. (2014). TZONE. [Online]. Available: at:tzonedigital.manufacturer.com
[27] H. J. Taha and M. F. M. Salleh, "Performance comparison of waveletpacket transform (WPT) and FFTOFDM system based on QAM modulationparameters in fading channels," *WSEAS Transactions Oncommunications*, vol. 9, no. 8, 2010.
[28] M. Roberti. (2014). *RFID Journal.* [Online]. Available: www.rfidjournal.com
[29] C. Seidler, "RFID opportunities for mobile telecommunication services," *ITU-T Lighthouse Technical Paper*, May 2005.

S. P. Majumder received his B.Sc. and M.Sc. Engg. (electrical and electronic) from BUET in 1981 and 1985 respectively. He completed his Ph.D. in electrical electronic and communication engineering (photonics) from Indian Institute of Technology (IIT), Kharagpur, India in the year 1991. His research interest includes opto-electronics and photonics, optical fiber communication systems, optical networks, solution propagation, satellite, mobile and infra-red communications.

He has worked as a research associate in University of Parma, Italy from June 1997 to August 1998. From December 2000 to March 2001, he has worked as a research professor in Gunma University, Tokyo, Japan. From January 1999 to July 2002 he has worked as the visiting professor at the Multimedia University, MMU, and Kuala Lumpur, Malaysia. He has published more than 70 research papers and authored/co-authored more than 75 conference papers. He has successfully completed a number of research projects sponsored by the European Commission, Telekom Malaysia and the Ministry of Science & Technology, Malaysia.

At present Dr. S.P Majumder is working as a professor in the Department of Electrical and Electronic Engineering, BUET, Dhaka, Bangladesh.

Khalid Mahmud was born in Jessore, Bangladesh on 16th September 1975. He received the bachelor of engineering degree in electrical and electronic engineering (EEE) from BUET, Dhaka, Bangladesh in 2004. He is currently working toward the M.Sc. degree in electrical and electronic engineering (communication) at the same university.

His research interests include RFID and wireless communication on which he has published a number of papers. He has worked as a technical staff in many organizations and educational institutions in Bangladesh Army.

At present Khalid Mahmud is working in Military Institute of Science and Technology, Dhaka, Bangladesh as an instructor class 'B' in the Department of Electrical Electronic and Communication Engineering (EECE).